Performances of Wang-Landau algorithms for continuous systems

P. Poulain

Laboratoire de Spectrométrie Ionique et Moléculaire, UMR 5579, Université Lyon I et CNRS, 43 Bd du 11 Novembre 1918, 69622 Villeurbanne Cedex, France

F. Calvo

Laboratoire de Chimie et Physique Quantiques, IRSAMC, Université Paul Sabatier, 118 Route de Narbonne, F31062 Toulouse Cedex, France

R. Antoine, M. Broyer, and Ph. Dugourd

Laboratoire de Spectrométrie Ionique et Moléculaire, UMR 5579, Université Lyon I et CNRS, 43 Bd du 11 Novembre 1918, 69622 Villeurbanne Cedex, France

The relative performances of different implementations of the Wang-Landau method are assessed on two classes of systems with continuous degrees of freedom, namely, two polypeptides and two atomic Lennard-Jones clusters. Parallel tempering Monte Carlo simulations serve as a reference, and we pay particular attention to the variations of the multiplicative factor f during the course of the simulation. For the systems studied, the Wang-Landau method is found to be of comparable accuracy as parallel tempering, but has significant difficulties in reproducing low-temperature transitions exhibited by the Lennard-Jones clusters at low temperature. Using a complementary order parameter and calculating a two-dimensional joint density of states significantly improves the situation, especially for the notoriously difficult LJ_{38} system. However, while parallel tempering easily converges for LJ_{31}, we have not been able to get data of comparable accuracy with Wang-Landau multicanonical sampling.

PACS number(s): 05.10.Ln, 02.70.Tt, 64.60.Cn, 65.40.Ba

I. INTRODUCTION

Many statistical and dynamical properties of complex systems can be related to the topography of their potential energy surface (PES), or energy landscape [1]. The degree of complexity itself depends on the number of basins, or inherent structures, on their distribution, and on their connectivity. In most cases, no obvious knowledge of the energy landscape characteristics can be guessed from the mere Hamiltonian, even though some universal features are expected based on catastrophe theory analyses [2]. Numerical exploration is thus an invaluable way of getting insight into the PES, provided appropriate simulation tools are used. Beyond the common Monte Carlo (MC) and molecular dynamics (MD) methods, a plethora of algorithmic improvements and sophisticated techniques [3] have led to major advances in fields such as phase transitions, glasses, or protein folding, to name a few. In the context of thermodynamical equilibrium, one faces the need for estimating statistical quantities, starting with the partition function, for instance, by sampling the relevant regions of the PES, that is the parts having a significant probability density. The sampling problem is particularly troublesome when the energy landscape has competing minima or when it is "rugged." Conventional MC or MD methods then become completely inefficient because they are unable to prevent the system from being stuck in a specific minimum, often dependent on the initial conditions. Given the restricted time and length scales available in molecular simulation, what should be physically seen as a slowing down of the dynamics is viewed here as kinetic trapping, or a case of broken ergodicity.

A series of methods have been proposed to alleviate such troubles by enhancing the exploration properties of Monte Carlo and molecular dynamics. The seminal idea of Torrie and Valleau [4] to bias the potential energy unphysically, in order to drive the system toward the desired regions of the PES is probably one of the most famous examples. Currently, two main categories of algorithms devoted to recovering ergodic sampling seem to be in use, namely, multiple replica strategies and broad-histogram methods. All of them belong to the so-called generalized ensemble class of methods.

The multiple-replica approach [5–10], also termed parallel tempering, considers performing several trajectories simultaneously, each trajectory being defined by a specific parameter (usually the temperature). Occasionally, exchange moves between a pair of trajectories or replicas are attempted, and accepted according to an appropriate Metropolis-like rule [3]. This method is particularly useful when the PES consists of multiple minima with comparable depths, as the random walkers can thus jump back and forth between minima. At present it has been widely accepted as a standard tool for accelerating convergence in simulation.

Broad-histogram [11] or flat-histogram [12–14] methods, among which the multicanonical ensemble sampling [12] stands as a landmark, seek to bias the energy of the system in such a way that all energies become equiprobable. The transition-matrix Monte Carlo approach of Wang and Swendsen [15] is a related method in which a stochastic matrix in the space of energies is computed during the simulation and postprocessed. If this histogram of visits is effectively flat, then the exploration of the PES is highly facilitated due to

the increased ease with which barriers are crossed. Unfortunately, the ideal biasing function is unknown at the start, since it would carry the exact same information as the density of states (DOS) of the system, which entirely characterizes its thermodynamics at equilibrium. Iterative schemes have been proposed to estimate the bias with increasing accuracy [12]. More recently, Wang and Landau (WL) suggested an interesting alternative way of reaching flat histograms, by constructing directly the DOS through dynamical update of the statistical weights entering the Metropolis acceptance rate. The generality, elegance, and apparent simplicity of the Wang-Landau method have led to a large variety of applications, ranging from magnetic systems [16–25], liquid crystals [26], fluids [27–31], biomolecules [32–37], atomic clusters [38,39], or structural [40] and spin [17] glasses.

The striking advantage of the WL method is its straightforward connection with the density of states, in addition to performing a random walk in energy space. Thus, it naturally achieves a multicanonical sampling, providing the DOS as a by-product. However, despite being generally regarded as very powerful, the Wang-Landau algorithm suffers from several drawbacks, especially when applied to continuous systems, that is systems with continuous degrees of freedom. These drawbacks stem from the difficulty of dealing with the boundaries of the accessible conformational space, as well as from the practical discretization of the energy range, which can pose significant problems when the DOS spans many orders of magnitude, as it occurs for large systems at low energy. Several improvements have recently been proposed in order to solve these difficulties [28,41–44].

In this paper, we aim at assessing the performance of the Wang-Landau method, and some of its offsprings, to correctly sample the configuration space of several continuous systems. We have chosen two polypeptides and two atomic Lennard-Jones (LJ) clusters as benchmarks. Even though these systems are not awfully large, they can pose important problems in conventional simulations. For polypeptide molecules, the sampling of their complex energy landscape generally provides a convenient testing ground for simulation methods. Concerning the two clusters (LJ_{31} and LJ_{38}), these systems are well known for their lack of ergodicity at low temperature, originating from the two-funnel character of their energy landscape [45]. For the polypeptides and clusters investigated here, parallel tempering Monte Carlo simulations were performed as a reference, and various implementations of the WL method for continuous systems were carried out. Particular attention was paid to the "f schedule," which is how the Wang-Landau multiplicative factor f varies during the course of the simulation. Although most of the results were obtained with one-dimensional densities of states with energy as the single variable, the two clusters appeared to be too difficult for this simple approach, and we had to turn to two-dimensional DOSs depending on energy and an extra order parameter.

In Sec. II, we briefly recall the main elements of the Wang-Landau method, along with the various improvements that we implemented, mostly, but not only, from others [26,42,43]. We give the details of our simulations and discuss our results in Sec. III, including a closer look at global

convergence issues and tunneling times, and finally conclude in Sec. IV.

II. IMPLEMENTATIONS OF THE WANG-LANDAU METHOD

The Wang-Landau method seeks to perform a random walk in energy space [16] and to provide an accurate estimate of the microcanonical density of states. In the WL method, the flat histogram of energies is achieved by penalizing states more and more as they are being visited. Following the original presentation [16], a function $g(E)$ is introduced. Initially set to 1 in the entire energy range, the method modifies $g(E)$ iteratively, so that it converges to the true density of states $\Omega(E)$. The histograms $h(E)$ of visited energies produced during a Wang-Landau simulation are expected to be flat. In practice, a flatness criterion is used to determine whether convergence has been reached or not, and then the simulation can proceed to refine the current estimate of the DOS at a better accuracy.

A fundamental ingredient in a Wang-Landau simulation is the modification factor f used to improve the accuracy of the function g at each Monte Carlo step. Initially, f is set to a value of 2 or more [16]. At a given value of f, a number of MC iterations are performed using moves that are appropriate to the system under study (spin flips, atomic moves, or torsion shifts, for instance). Each MC move is accepted following a Metropolis rule:

$$\mathrm{acc(o \rightarrow n)} = \min\left[1, \frac{g(E_\mathrm{o})}{g(E_\mathrm{n})}\right] = \min\{1, \exp[s(E_\mathrm{o}) - s(E_\mathrm{n})]\},$$

(1)

in which we have noted the energies of the old (o) and new (n) configurations by E_o and E_n, respectively. We have also introduced the function $s(E) = \ln g(E)$, similar to an entropy, which is used in practice in order to avoid handling numbers having orders of magnitude that are too large.

Obviously, since g is set to 1 at the beginning, the above procedure will lead to all states being accepted, without producing any useful information. The trick in Wang-Landau simulations is that $g(E_\mathrm{n})$ is *modified* after the move has been performed, by multiplying it by f [16]. Equivalently, $s(E_\mathrm{n})$ is updated by adding $\ln f$ to it. In case the move was rejected, the old configuration is copied as the new one and the same rule applies. In both cases, the histogram of visits is updated by 1 at the corresponding energy.

Once a sufficient number of steps have been performed, the factor f is decreased exponentially (typically by taking $\sqrt{f} \rightarrow f$) and the simulation proceeds, starting for $g(E)$ with the last estimate at the previous iteration. Finally, the simulation ends after $\ln f$ has reached a sufficiently low value, the density of states being thus known to an accuracy no better than f. The convergence of the function g between two successive iterations can be monitored by looking at the flatness of the histogram of visits. In the original algorithm, the histogram was considered to be flat if all accessible states were populated by more than 95% of the average number of visits [16]. However, this criterion often appears to be too restric-
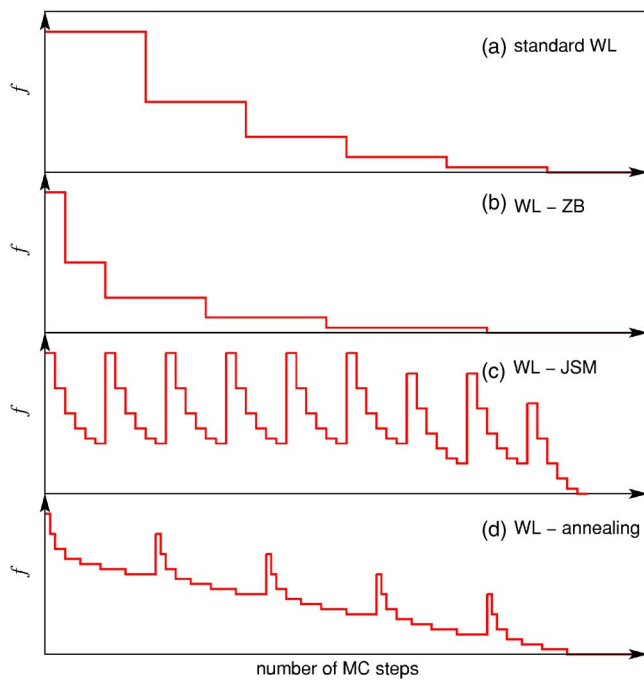
FIG. 1. (Color online) Schematic schedule of the variations of the modification factor f during the course of different Wang-Landau simulations. (a) Standard WL; (b) WL with Zhou-Bhatt condition (WL-ZB); (c) WL with Jayasri-Sastry-Murthy (WL-JSM) schedule; (d) WL-annealing schedule. See text for details about the ZB condition and JSM method.

tive, and usually a fixed number of hits on each energy bin are performed [28]. In many cases, a predefined maximum number of MC steps for each iteration is required, as illustrated in Fig. 1(a).

Several authors [17,28] have suggested dividing the available energy range into contiguous subdomains, possibly taking into account the different entropies of the various windows [28]. This strategy is well suited to parallel computing but may become risky if important energy barriers in one window prevent the system from properly equilibrating in domains having a lower energy. Another early improvement of the Wang-Landau method was to consider the moves that fall out of the accessible boundaries [42]. In such cases, Schulz et al. suggested to update the density of states and histogram of visits at the old configuration [42].

A more significant qualitative improvement was the study by Zhou and Bhatt (ZB) who showed that convergence of the function $g(E)$ toward the true DOS scales as $\sqrt{\ln f}$ [43]. In practice, a good convergence criterion in simulations could thus be that each bin is visited at least a number of times scaling with $1/\sqrt{\ln f}$.

Simulation of systems with continuous degrees of freedom can present extra difficulties, particularly when the energy landscape is rugged and hard to sample in its entire range [44]. Some regions of the DOS could be very narrow in configuration space, and this would result in the system being trapped in these regions without being able to escape because of the gap in DOS that it would have to fill. Such an accumulation problem is more likely to happen when dealing with a multidimensional (or joint) density of states, depend-

ing on one or several order parameters in addition to energy. Tröster and Dellago recently suggested to run a preliminary WL calculation, in order to delimit the practical range of available states [44]. Because of such accumulation problems, the convergence criterion based on a minimum number of visits being at least $1/\sqrt{\ln f}$ is often very hard to achieve, except for simple systems. Therefore, it becomes more convenient to convert this rule into a maximum number of steps prescription, namely, that the number of MC steps should be proportional to $1/\sqrt{\ln f}$. We will refer to this modification of the conventional WL scheme as the WL-ZB scheme, as illustrated in Fig. 1(b).

Other strategies have been proposed for addressing accumulation problems. Zhou et al. [46] have implemented a "global update" stage in which the current estimate of the DOS is partially scaled to higher values in order to favor exploration of the undersampled regions. These authors also designed a specific procedure for dealing with the continuous character of the degrees of freedom by working with continuous functions that spread over several bins instead of the steplike updates in a single bin [46].

The strategy described by Jayasri, Sastry, and Murthy (JSM) [26] differs significantly from the previous one; its variations of the modification factor are depicted in Fig. 1(c). In their work on lattice liquid crystals, Jayasri et al. divided each WL iteration into many substages. The modification factor f is only slightly decreased after each substage (typically $f^{0.9} \rightarrow f$), and takes its large initial value back after a number of substages have been performed. After several iterations, the starting value for f is decreased to achieve a better precision [26]. The strength of the WL-JSM method is that it allows f to vary nonmonotonically during the course of the simulation. As a consequence, gaps in the density of states can be more easily filled and accumulation is avoided.

Although increasing f back to its initial value at the previous iteration helps in driving the system out of possible entropic bottlenecks, it also destroys the accuracy with which the DOS was known. In the original implementation by Jayasri et al. [26], 50 WL iterations were performed, dividing each of them into 150 substages. The 40 first iterations started with $f=100$, the next nine with $f=10$, and the last refining iteration used $f=e^1$ at the beginning. Thus, in this method, the DOS becomes only accurate at the very end.

We have tried to combine several appealing features of the previous methods into a simple and general way of conducting Wang-Landau simulations. First, we keep the JSM idea of increasing the modification factor f occasionally, but we do not allow f to equal or to exceed its previous initial value. We follow a scheme for f similar to the variations of temperature during a simulated annealing optimization [47], as depicted in Fig. 1(d), and we will denote our method as "WL-annealing" (or WLA) in the following.

The WLA simulation is again organized into M main iterations, each of them being divided into N substages. The initial modification factor f decreases after each substage by $f^\alpha \rightarrow f$ with $\alpha < 1$. At the beginning of the next iteration, f is increased by $f^{1/\alpha^{N-1}} \rightarrow f$. If we denote by f_0 the initial modification factor at the beginning of the first iteration, then the last value at the end of the last substage of the last iteration will be $f_0^{\alpha^{M+N-2}}$.

Second, in order to account for the increasing need for statistics as f decreases, we also follow the prescription of Zhou and Bhatt [43] and scale the length of each substage according to $1/\sqrt{\ln f}$. This way we spend more time constructing the DOS as the simulation proceeds, but also getting a more and more accurate estimate.

Our implementation differs from the implementations of the original Wang-Landau scheme [16], as well as those by Zhou and Bhatt [43] and Jayasri *et al.* [26] from the way f varies during the simulation, or the f schedule. These differences are particularly prominent on the schematic representations of Fig. 1.

Obviously, the different f schedules can be further combined with other modifications, such as those aforementioned. However, for the systems studied below, we have not found significant improvements by using the approaches recommended for continuous systems by Zhou *et al.* [46], including global updates. Neither have we used *a priori* information about the accessible range of states by performing a preliminary WL run [44]. Yet we have dealt with moves falling off the boundaries in a similar way as Schulz *et al.* [42].

III. RESULTS

We have performed Wang-Landau simulations using several schemes for the f modification factor presented in Sec. II. The function $g(E)$ obtained at the last WL iteration provides an estimate of the true density of states $\Omega(E)$. Alternatively, the DOS can be determined from parallel tempering Monte Carlo simulations, by analyzing the distributions of potential energies of all replicas, using a standard histogram reweighting procedure [48]. We have performed such calculations with high statistics as a reference. The temperatures of the replica trajectories were determined so as to follow a geometric progression, as this scheme is (close to) optimal for parallel tempering simulations of classical continuous systems [49–52].

For both Wang-Landau and parallel tempering methods, the canonical thermodynamical quantities, such as the internal energy $U=\langle E \rangle$ or heat capacity $C=(\langle E^2 \rangle - \langle E \rangle^2)/k_B T^2$, are calculated by Laplace transformation of the density of states

$$\langle E^n \rangle = \frac{1}{Z} \int E^n \Omega(E) \exp(-\beta E) dE; \qquad (2)$$

$$Z = \int \Omega(E) \exp(-\beta E) dE, \qquad (3)$$

with $\beta = 1/k_B T$.

Equilibrium distributions $p(\lambda)$ or thermal averages $\langle \lambda \rangle$ of a physical observable λ not depending directly on energy must be obtained differently, by recording the two-dimensional histogram of visited (E, λ) states, thus keeping the correlations between E and λ [53]. In practice, the microcanonical density of states $\Omega(E)$ from either a Wang-Landau simulation or from a parallel tempering simulation provides the biasing function to a subsequent multicanonical

simulation in which the histogram $\widetilde{h}(E, \lambda)$ is computed (here the tilde notation indicates the multicanonical bias). Standard reweighting formulas are then used to calculate $\langle \lambda \rangle$ as

$$\langle \lambda \rangle = \frac{1}{\widetilde{Z}} \int \int \lambda \widetilde{h}(E, \lambda) \Omega(E) \exp(-\beta E) dE d\lambda, \qquad (4)$$

$$\widetilde{Z} = \int \int \widetilde{h}(E, \lambda) \Omega(E) \exp(-\beta E) dE d\lambda. \qquad (5)$$

The multicanonical simulation based on the density of states obtained from different methods (parallel tempering and one-dimensional WL) is also insightful, because the quality of the DOS can be probed from the flat-histogram dynamics generated by these methods.

The extra multicanonical calculation for obtaining $\langle \lambda \rangle$ in a continuous temperature range is not needed if the histogram $h(E, \lambda)$ of visited states is computed during the parallel tempering simulation, or if the Wang-Landau simulation is performed using the two variables E and λ instead of simply E, thus providing a joint density of states $\Omega(E, \lambda)$. The canonical average $\langle a \rangle$ of any property a depending on E and λ can then be recovered using the following reweighting formulas:

$$\langle a \rangle = \frac{1}{\hat{Z}} \int \int a(E, \lambda) \Omega(E, \lambda) \exp(-\beta E) dE d\lambda, \qquad (6)$$

$$\hat{Z} = \int \int \Omega(E, \lambda) \exp(-\beta E) dE d\lambda. \qquad (7)$$

A. Polypeptides

Many challenges in computational biology originate from the huge need in simulation methods and computer power. Although real proteins can sometimes be directly simulated [54], loads of problems are still waiting for solutions: protein folding, drug-protein binding, etc. On the route toward the increasing complexity of such systems, peptides appear as convenient models that can help in the understanding of larger biomolecules. Our systems of interest are the polypeptides Ala_8 and $[Ala-Gly-Trp-Leu-Lys+H]^+$ (AGWLK$^+$). The polyalanine molecule is convenient for the study of the helix-coil transition [55,56]. AGWLK$^+$ is an experimentally designed model peptide used in the study of laser or collision-induced dissociations [57,58]. This molecule shows different fragmentation behaviors depending on its charge state being +1 or +2. These differences have been attributed to changes of conformation [58]. Both peptides are simulated in the gas phase with the all-atom AMBER force field [59] with *ff96* parameters [60] and a dielectric constant of $\varepsilon = 2$.

Parallel tempering simulations were carried out with 19 replicas between 100 and 1100 K for Ala_8 and with nine replicas between 180 and 1100 K for AGWLK$^+$. The temperature repartitions follow a geometric progression [49–52]. A Monte Carlo sweep consists of randomly perturbing each dihedral angle in the peptide backbone (including Φ and Ψ angles) and in the side chains once. Bond lengths and bond

angles are kept constant. The simulation for Ala_8 was run for 6.2×10^9 Monte Carlo steps with 6.2×10^8 Monte Carlo steps discarded for thermalization, summed for all replicas. This represented about 48 h of calculation on a 2.6 GHz AMD Opteron Intel processor . The simulation for $AGWLK^+$ was run for 6.8×10^8 MC steps with 6.8×10^7 MC steps of thermalization, representing ~ 12 h of computer time on a 2 GHz Intel Xeon processor.

Different implementations of the WL algorithm have been performed following the modification factor schedules depicted in Fig. 1. All simulations started with $f_0 = e^1$ and ended with the same final accuracy such that $\ln f \simeq 2 \times 10^{-6}$. The accumulated computational cost was identical for each method, namely 4.2×10^8 MC steps for Ala_8 and $AGWLK^+$.

In the original implementation of the WL algorithm and in the implementation using the ZB condition, 20 iterations are performed, the number of steps per iteration being only dependent on f in the latter case. The JSM implementation consists in 50 iterations and 85 substages per iteration. The 40 first iterations started with $f_0 = e^1$, the next nine with $f_0 = e^1/10$, and the last one with $f_0 = e^1/100$. Following Ref. [26], the modification factor is updated by $f^{0.9} \rightarrow f$ after each substage. Our WL-annealing implementation is composed of 16 iterations and 5 substages. The factor f is updated by taking $f^{0.5} \rightarrow f$ as in the original WL implementation [16,17]. For all WL simulations, the energy range was discretized in 400 bins for both Ala_8 and $AGWLK^+$.

Typical heat capacities obtained from parallel tempering and Wang-Landau simulations are depicted in Fig. 2 for the two polypeptides. For Ala_8, the heat capacity shows a main peak near 250 K, which is comparable to results obtained for Ala_{10} by other authors [61,62]. Only the WL-annealing simulation properly reproduces the entire curve and the observed peak, even with fewer MC steps than the parallel tempering calculation. Both the standard WL and WL-ZB clearly differ, overestimating and underestimating the transition temperature, respectively. The most important disagreement is found for the JSM implementation, which seems to fail for this system.

The heat capacity of $AGWLK^+$ does not exhibit a peak as sharp as the one for the polyalanine molecule. Here the transition connects the ground state to the coil state much more continuously, as can be expected from the smaller size of this polypeptide. Again, the WL-annealing scheme compares best to the parallel tempering data, with a similar number of MC steps. Standard WL and the WL-ZB implementation are now in much closer agreement, but the JSM schedule remains poorly efficient in terms of global convergence of the heat capacity.

The previous WL calculations have been repeated several times, and we were not able to obtain a better agreement with parallel tempering data at comparable numerical cost, except when using the present annealing schedule. In particular, we tried to vary the numbers of main iterations and substages of the JSM implementation, as well as the rate of decrease of the modification factor, without obtaining significantly better results. Therefore, the WL-annealing scheme seems to perform best with respect to the other f schedules, at least on the two present polypeptide systems.

We also calculated the thermal average $\langle d \rangle$, d being the distance between the tryptophan indolic nitrogen and the
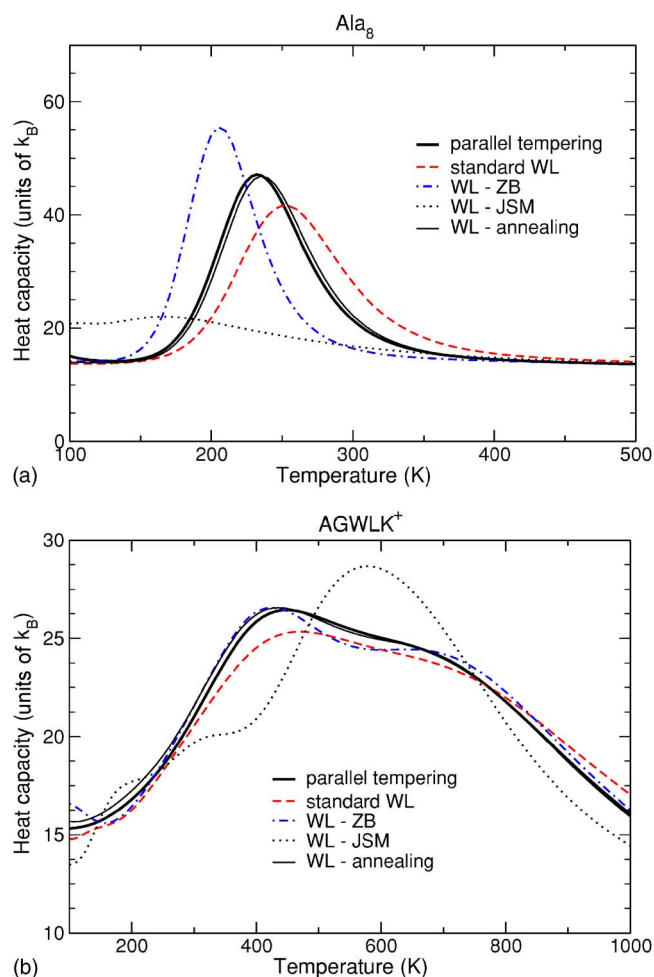
FIG. 2. (Color online) Heat capacity curves of gas-phase polypeptides, as a function of temperature. The results of various implementations of the Wang-Landau method are compared to the data obtained with parallel tempering Monte Carlo. (a) Ala_8, (b) $AGWLK^+$.

protonated nitrogen of the lysine amino acid of the $AGWLK^+$ polypeptide (this represents a measure of the extension of the peptide). For this, an extra multicanonical simulation was performed in order to calculate the histogram $\tilde{h}(E,d)$ as explained previously. A total of 1.5×10^9 configurations were generated using the density of states $\Omega(E)$ obtained from the WL-annealing algorithm. Figure 3 shows the variations of $\langle d \rangle$ with temperature calculated directly from parallel tempering (with and without histogram reweighting) and from multicanonical simulation with the DOS obtained from the WL-annealing calculation. $\langle d \rangle$ shows a monotonic increase, which is strongest at the temperature where the heat capacity exhibits its maximum value. Thus, the distance d provides a convenient probe of the folding phase change in $AGWLK^+$. The good agreement obtained between the two computational methods indicates that our implementation of the Wang-Landau algorithm is competitive with exchange Monte Carlo for the present system.
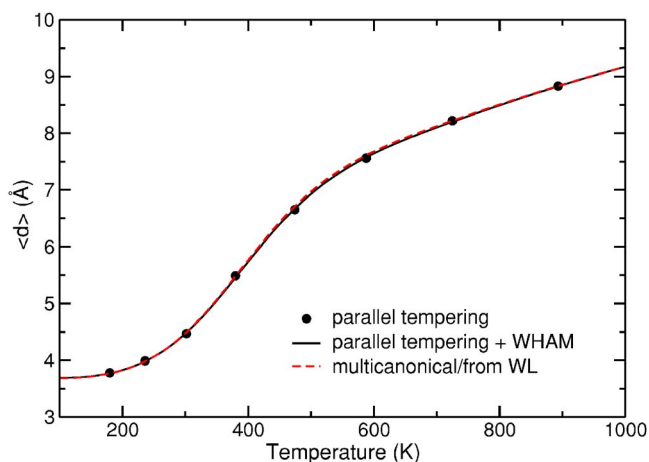
FIG. 3. (Color online) Thermal average $\langle d \rangle$ of the distance between the tryptophan indolic nitrogen and the protonated nitrogen of the lysine amino acid of the AGWLK$^+$, obtained from parallel tempering and multicanonical simulations. The density of states of the multicanonical simulation is provided by the WL-annealing method. For the parallel tempering data, both the direct results at the replica temperatures (symbols) and the continuous variations after histogram analysis are shown.

B. Lennard-Jones clusters

Clusters of N Lennard-Jones atoms have often been used as benchmarks for statistical studies, including optimization and sampling problems [63–66]. Due to their multiple-funnel energy landscape [67], some of these clusters represent a significant challenge for ergodic simulation. Until now, parallel tempering Monte Carlo has remained the most robust method to simulate directly the solid-solid transition in clusters, such as LJ$_{31}$ [68,69], LJ$_{38}$ [70–72], or more recently LJ$_{75}$ [73]. Although most LJ clusters usually show fivefold symmetries and icosahedral shapes below 100 atoms [65], some specific sizes are more stable in other kinds of geometries, such as octahedral (LJ$_{38}$) or decahedral (LJ$_{75}$). However, icosahedral structures are only marginally higher in energy, but they also have a higher entropy; therefore, a structural transition takes place at temperatures below the melting point [74]. In the case of LJ$_{31}$, the structural transition involves two icosahedral phases, corresponding to a single layer, 13-atom icosahedron with different overlayers [75].

For LJ clusters, all simulations have been performed using a hard-wall confining sphere to prevent dissociation. The radii chosen are 2.5 and 2.8 LJ reduced units for LJ$_{31}$ and LJ$_{38}$, respectively.

Parallel tempering simulations were conducted in the reduced temperature ranges $0.01 \leqslant k_B T/\varepsilon \leqslant 0.45$ for LJ$_{31}$ and $0.01 \leqslant k_B T/\varepsilon \leqslant 0.35$ for LJ$_{38}$, using 50 replicas and a geometric progression. A total of 5×10^9 MC steps have been included in the statistical averages, taken from the same number of MC sweeps and after 10^8 cycles of thermalization. On a serial 2.2 GHz Opteron processor, this represented about one week of calculation for LJ$_{38}$ and four days for LJ$_{31}$. The Q_4 and Q_6 order parameters introduced by Steinhardt *et al.* [76] to distinguish different local orders in bulk

matter have been calculated to quantify the probability of visiting the global minimum funnel. Thus, these quantities provide a direct connection with the solid solid transition. By definition, Q_4 and Q_6 are given as

$$Q_\ell = \left(\frac{4\pi}{2\ell + 1} \sum_{m=-\ell}^{\ell} |\bar{Q}_{\ell m}|^2 \right)^{1/2}, \qquad (8)$$

with

$$\bar{Q}_{\ell m} = \frac{1}{N_b} \sum_{r_{ij} < r_0} Y_{\ell m}(\theta_{ij}, \phi_{ij}). \qquad (9)$$

In Eq. (9), the sum is over all pairs of atoms whose distance r_{ij} is lower than a nearest-neighbor criterion r_0. There are N_b such pairs in the cluster, and the value $r_0 = 1.3909$ LJ units is used here. $Y_{\ell m}(\theta, \phi)$ is a spherical harmonic and θ_{ij} and ϕ_{ij} are the polar and azimuthal angles of an interatomic vector with respect to an arbitrary coordinate frame. Although Q_4 and Q_6 will be used for LJ$_{38}$ and LJ$_{31}$, respectively, we denote them both as Q for generality below.

We have implemented the Wang-Landau method with the same f schedules as discussed in Sec. II, but only results obtained with the WLA scene will be discussed hereafter. In accordance with our results on polypeptides, we generally found that the annealing schedule provides a faster convergence for the DOS with respect to other schemes.

Fifty main WL iterations have been performed with a starting modification factor $f_0 = e^1$, and for each iteration 100 substages were conducted by taking $f^{0.9} \to f$ after each substage. The number of MC cycles per substage was taken as $10^4/\sqrt{\ln f}$. For the one-dimensional calculations of the density of states, the energy range was divided into 1000 equal bins. Two-dimensional calculations have also been carried out, using 200 energy bins and 100 bins in the Q order parameters. As aforementioned, the one-dimensional WL method in energy space only does not provide information about the order parameters, and an extra multicanonical simulation has to be performed using the density of states obtained from either Wang-Landau or parallel tempering simulations. The thermal averages $\langle Q \rangle$ were evaluated from the reweighting formula, Eq. (4). For consistency, the heat capacities shown below and referring to the one-dimensional WL-annealing method are actually the outcome of the same multicanonical simulation, the curves directly obtained from the Wang-Landau DOS not being significantly different.

The heat capacities and variations of the thermal average of Q_4 are represented in Fig. 4 for LJ$_{38}$. The heat capacity shows one main peak near $k_B T/\varepsilon = 0.17$, indicative of melting [72,77]. The shoulder on the low-temperature side of this peak reflects the solid-solid transition between the octahedral global minimum and the icosahedral structures. The solid-solid transition temperature T^* can be inferred from the variations of $\langle Q_4 \rangle$, which strongly drop at $k_B T^*/\varepsilon \simeq 0.11$.

The Wang-Landau annealing calculation (followed by a multicanonical extra stage), with a comparable number of MC steps as the parallel tempering simulation, correctly reproduces most of the caloric curve, including the main melting peak. However, it significantly overestimates the solid-
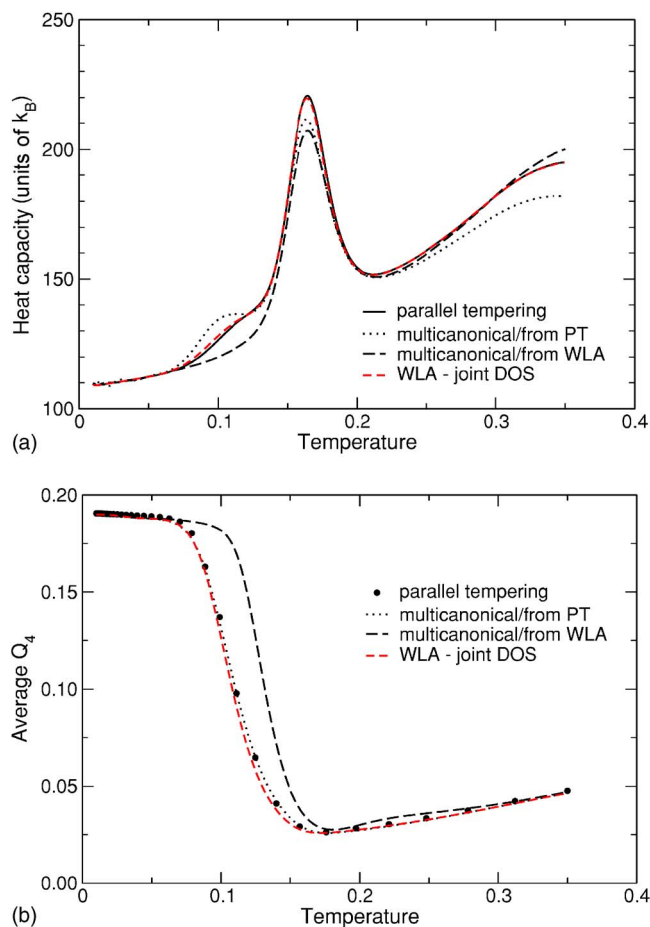
FIG. 4. (Color online) Thermodynamical and structural data for the LJ_{38} cluster obtained from parallel tempering, from multicanonical simulations using the density of states from parallel tempering or from WL-annealing simulations, and from two-dimensional WL-annealing simulations. (a) Heat capacity, (b) $\langle Q_4 \rangle$ order parameter. The temperature is given in reduced LJ units of ε/k_B.

solid transition temperature, as seen from both the absence of any shoulder in the heat capacity and the delayed decrease in $\langle Q_4 \rangle$. To determine whether this poor agreement with parallel tempering comes from the initial WL simulation or from the subsequent multicanonical stage, we have repeated the multicanonical simulation, but starting from the density of states obtained by multihistogram analysis of the energy distributions in parallel tempering. The heat capacity and the order parameter are now much closer to the original parallel tempering data. This shows that the multicanonical simulation had enough time to converge, but also that the one-dimensional WL-annealing simulation could not reproduce the equilibrium between the two octahedral and icosahedral funnels. However, the success of multicanonical sampling for this system, when initiated properly with a high-quality DOS, is encouraging for pure Wang-Landau sampling, even though it suggests that a much larger number of steps, or new improvements to the method, should be incorporated.

In a first approach, the poorer convergence of the Wang-Landau calculation can be explained by the necessity for the single walker to cross the interfunnel barrier many times, while instantaneous swap moves are performed in parallel

tempering. An inspection of the average tunneling events between the first five and last five bins of the entire energy range, denoted as L and H, respectively, shows that only about 10 L→H events (and as many H→L events) occur during the entire simulation, with an average tunneling time of 2×10^6 MC cycles for both L→H and H→L directions. Such a long time prevents reasonably good statistics from being obtained. The much greater probability of finding the entropically dominant icosahedra reveals that the walker has higher chance of going back to the icosahedral funnel than from effectively crossing the barrier. This effect is magnified by the cooperative nature of the icosahedral-octahedral rearrangement [78].

Using an extra order parameter for the DOS may help to bypass barriers. We have thus performed a WL-annealing calculation to obtain the joint density of states $\Omega(E, Q_4)$, using the very same schedule for the modification factor as in one-dimensional WL simulations. The heat capacity and the thermal $\langle Q_4 \rangle$ have then been calculated using the reweighting formula of Eq. (6). Both quantities are now in very good agreement with the parallel tempering results. This agreement shows that not only the use of the Q_4 order parameter is crucial for a successful flat-histogram sampling, but also that the Wang-Landau annealing can be of comparable efficiency to parallel tempering. By defining the octahedral and icosahedral regions according to their low energy and high or low values of Q_4, respectively, we have estimated the tunneling times in the joint DOS calculation, finding now about 500 events. This larger number is a good manifestation that sampling between the two funnels was more successful this way.

We now turn to the smaller cluster LJ_{31}. Even though our simulations were performed with the same statistics as for LJ_{38}, our experience shows that convergence of parallel tempering is achieved faster for the smaller cluster. This is likely to be related to the lower barriers between the anti-Mackay and Mackay funnels with respect to those between the octahedral and icosahedral funnels of LJ_{38} [45].

For the LJ_{31} cluster, Q_6 exhibits significantly different values between the anti-Mackay and Mackay isomers, and provides a suitable order parameter to distinguish between the low-temperature states [79]. The heat capacities and thermal variations of $\langle Q_6 \rangle$, as obtained from parallel tempering and Wang-Landau annealing simulations, are represented in Fig. 5.

Similarly to LJ_{38}, the heat capacity of LJ_{31} displays two peaks, one broad peak near $k_B T/\varepsilon \simeq 0.32$ characteristic of the melting transition and one rather narrow peak at very low temperature $k_B T^*/\varepsilon \simeq 0.03$ [68,69]. This narrow peak is the signature of the Mackay to anti-Mackay structural transition from the global minimum to structures higher in both energy and entropy. The higher valuer of Q_6 for the Mackay isomers helps visualizing the transition in Fig. 5(b).

As was the case for LJ_{38}, the one-dimensional WL-annealing simulations globally reproduce most of the heat capacity curve at moderate or high temperatures, including the broad melting peak. After performing the extra multicanonical simulation, the thermal variations of $\langle Q_6 \rangle$ are in agreement with those from parallel tempering, but only for temperatures above T^*. The WL-annealing method fails in
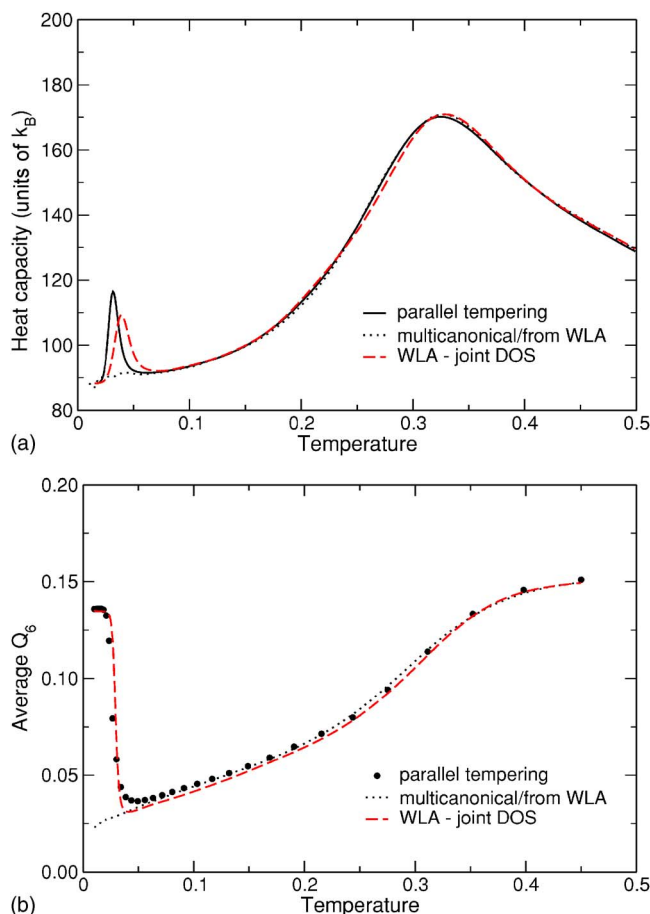
FIG. 5. (Color online) Thermodynamical and structural data for the LJ_{31} cluster obtained from parallel tempering, from multicanonical simulations using the density of states from WL-annealing, and from two-dimensional WL-annealing simulations. (a) Heat capacity, (b) $\langle Q_6 \rangle$ order parameter. The temperature is given in reduced LJ units of ε/k_B.

correctly sampling the funnel of the global minimum, as seen from the steady increase of the order parameter at low temperatures. We repeated the multicanonical simulation using the density of states obtained from parallel tempering and subsequent histogram reweighting. Unfortunately, the curves (not plotted here) did not show any notable differences with respect to those obtained using the Wang-Landau estimate of the DOS. The multicanonical simulation is clearly unable to achieve a flat histogram in the low-energy end of the available range. The reason for that is likely the same as those that prevented a full equilibration for the WL sampling of LJ_{38}, namely, the difficulty to cross the barrier separating the two funnels. The initial Wang-Landau simulation, which proceeds in a way very close to multicanonical sampling, also suffers from the very rare crossing events, resulting in a limited sampling of the global minimum. The near-degenerate energies of the bottom of the two funnels make the situation even worse than in LJ_{38}, because the measured tunneling times, computed from the energy spanned alone, cannot tell whether the global minimum funnel was actually visited.

There are about as many tunneling events in the multicanonical simulation of LJ_{31} as there were for LJ_{38}, namely,

about 10 $L \rightarrow H$ events and 10 $H \rightarrow L$ events, with an average tunneling time close to 10^6 MC cycles. However, these events correspond to transitions between high-energy configurations and anti-Mackay structures rather than the global minimum. A much more strict criterion for detecting tunneling events that could probe the global minimum would require looking at the very first energy bins, which are below the minimum energy of the second funnel. Using this criterion, only a single $H \rightarrow L$ event was seen during the entire multicanonical simulation of LJ_{31}. In this case, the original criterion of Zhou and Bhatt [43] that the minimum number of visits per bin should scale as $1/\sqrt{\ln f}$ could lead to extremely slow convergence, that is, unless the bin size is increased, in which case the resolution of the DOS might not be high enough to correctly reproduce the solid-solid transition.

Thus, the extra difficulties found for multicanonical sampling of the low-energy parts of the landscape of LJ_{31}, even when supplied with an accurate density of states, probably reflects the very narrow energy range over which the structural transition takes place (only a few bins out of 1000). Following Shell *et al.* [28], we tried to solve this problem by sampling energy bins according to the expected entropy of these bins, using an approximate logarithmic variation for the bin width. However, this resulted in even poorer convergence of the initial WL calculation and a rather bad agreement with parallel tempering over a broader temperature range.

Using Q_6 as an extra order parameter in a joint-DOS approach, the Wang-Landau annealing simulation now performs significantly better. In particular, the variations of $\langle Q_6 \rangle$ with temperature match the parallel tempering results very satisfactorily. The low-temperature peak of the heat capacity is also present, albeit slightly broader and shifted to a higher temperature. Tunneling between the anti-Mackay and Mackay isomers, defined according to both their low energy and a low or high value of Q_6, respectively, is now facilitated, about 100 events being found.

In the present case of LJ_{31}, the joint-DOS WL-annealing simulation seems to have reached a better convergence. However, as far as numerical accuracy is concerned, a parallel tempering calculation performed with one order of magnitude fewer MC steps than the WL simulation produces nearly the same heat capacity curve.

C. Global convergence and tunneling times

For spin systems, such as the Ising model, the tunneling time between the lower and upper ends of the energy range provides a convenient way of measuring the performance of sampling algorithms because energy itself can be used as an order parameter for the ordered phases. The performance of the Wang-Landau method to generate flat-histogram dynamics on such systems, as inferred from its distribution of tunneling times, has been investigated by Dayal *et al.* [80]. In case of a simple energy landscape, or for systems not exhibiting any phase transition, short tunneling times are also a good indication that the flat-histogram method was successful [81].
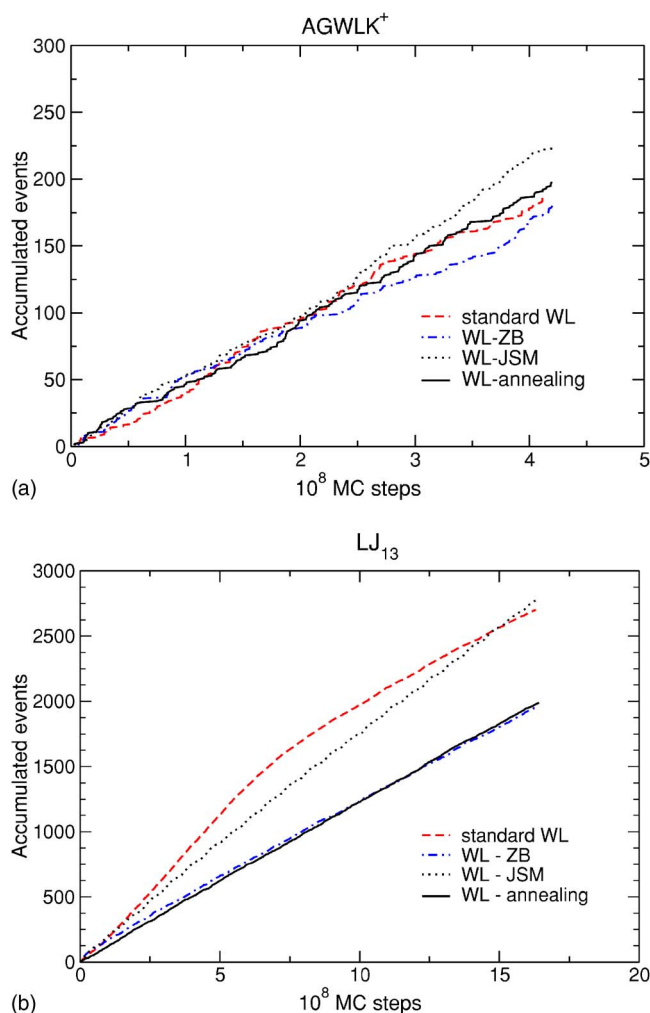
FIG. 6. (Color online) Accumulated number of L→H tunneling events for different implementations of the Wang-Landau method, during the course of the simulations. (a) AGWLK$^+$, (b) LJ$_{13}$.

In a recent analytical study [82], Costa *et al.* showed that multicanonical sampling should not produce equal tunneling times between regions with low and high entropy, respectively, the time needed to go back into regions with low entropy being significantly longer. The nonequivalence between equilibration time and tunneling time was also critically discussed by these authors [82].

In the two examples of biomolecules investigated previously, we chose to monitor global convergence of Wang-Landau samplings on the thermodynamical observables. We also computed the tunneling times needed for crossing the entire energy range from the low to high values (L→H process) or the reverse (H→L), the first five and last five bins of the physically accessible energy range being used as an arbitrary definition of the L and H states, respectively. The variations of the number of L→H tunneling events as the Wang-Landau simulations progress are represented in Fig. 6(a) for the AGWLK$^+$ polypeptide. Because the number of tunneling events remains quite small with all methods, we also performed additional simulations for the simpler LJ$_{13}$ cluster. In both cases, the simulations are compared at a fixed total computational cost.

Even though AGWLK$^+$ and LJ$_{13}$ are very different systems, the four methods seem to behave similarly for them. Quite strikingly, the rate of tunneling events is highest for the JSM implementation of the WL method, then for the standard WL method, and finally for the methods using the Zhou and Bhatt prescription on the number of steps. The initial stages of the WL dynamics, thus, play an important role as they contribute to shape the global variations of the DOS, which, in turn, leads to an efficient random walk in energy space. However, the poor correlation between the number of tunneling times and the quality of the heat capacities calculated with the corresponding density of states indicates that, even though tunneling events may be numerous and fast, the quantitative accuracy of the DOS may not be as good.

IV. CONCLUDING REMARKS

Sampling the energy landscape is a difficult but important task in many areas of statistical and chemical physics, ranging from supercooled liquids, spin glasses to clusters, and biomolecules. In the present work, we investigated the sampling efficiency of various implementations of the Wang-Landau method to systems for which parallel tempering usually converges well. We have especially focused on the *f* schedule, that is how the modification factor varies during the course of the simulations. We have generally found that combining the ideas of Zhou and Bhatt [43] and those of Jayasri *et al.* [26] works best for the present case studies. The resulting Wang-Landau annealing schedule that we propose here is a general way of performing a random walk in energy space that significantly helps in avoiding accumulation in low energy-bins.

However, even though the WL-annealing scheme was seen to improve over other implementations of the Wang-Landau method, notable difficulties were met in the case of Lennard-Jones clusters characterized by a two-funnel energy landscape. These difficulties essentially appear at low energies, the random walker having trouble to cross the energy barrier between the two main funnels. We found that employing a suitable order parameter in a joint DOS calculation contributes to a better sampling of the two low-temperature equilibrium states, yielding much more satisfactory thermodynamical and structural results. Only at this cost, did the Wang-Landau annealing simulation become competitive with parallel tempering in terms of numerical cost and overall exploration efficiency.

We tried to further improve the Wang-Landau algorithm by supplementing it with the ideas recently advocated by Zhou *et al.* [46]. Working with continuous instead of stepwise functions is very appealing, but we had significant trouble in converging the density of states at the very low energies, due to the rather soft behavior of the Gaussian or parabolic functions used in Ref. [46] with respect to the expected, steep variations of the DOS [ln $\Omega(E) \propto \ln(E - E_0)$ for $E \to E_0^+$]. The global update scheme suggested in the same paper [46] was also implemented, but we found hard to determine, in advance, what the threshold should be above which the DOS should be scaled.

Our experience on the Wang-Landau methodology confirms that the method is usually powerful and can even com-

pete with parallel tempering in difficult cases where the energy landscape is made of several low-temperature basins. However, although the method is general, we believe that tuning its various parameters is an important stage of the simulation. Apart from some general considerations about the scaling of the number of MC steps with the modification factor or the f schedule itself, the values that should be adopted for the initial value of f, its decreasing rate α after each new iteration, and the numbers M and N of iterations and substages may be highly system dependent. The number of parameters to be set in parallel tempering is comparatively much less, especially if simple but efficient rules for the repartition of temperatures are chosen.

While using extra order parameters to help circumventing barriers can have important benefits, these should also be balanced with the choice of order parameters, as well as the increasing size of the histograms resulting from adding as many parameters. In particular, visiting all states of a multi-dimensional parameter state becomes more and more demanding as new order parameters are used.

Another conclusion reached in the present study is that the tunneling times between the two boundaries of the available energy range, as calculated during the course of the Wang-Landau calculation, may not be a good signature of the degree of accuracy reached by the density of states. This was particularly critical in the base of the AGWLK$^+$

polypeptide, which yielded the fastest tunneling times, but for which we were not able to get globally converged heat capacities. This quite unexpected result agrees with the conclusion by Costa *et al.* [82] that equilibration times and tunneling times, though related, may differ significantly.

Finally, we should emphasize that, although they represent nontrivial simulation case studies, the systems chosen here all have a relatively small number of degrees of freedom that allow parallel tempering calculations to converge ideally. Much larger systems will make the parallel tempering strategy less useful, because the distributions of visited energy between adjacent replicas will have a smaller overlap; hence, the swapping efficiency will be drastically reduced. The Wang-Landau method could then offer a quantitative estimate of the density of states at a much better numerical cost than replica-based approaches.

ACKNOWLEDGMENTS

[1] D. J. Wales, *Energy Landscapes* (Cambridge University Press, Cambridge, England, 2003).

[2] D. J. Wales, Science **293**, 2067 (2001).

[3] D. Frenkel and B. Smit, *Understanding Molecular Simulation*, 2nd ed. (Academic Press, London, 2002).

[4] G. M. Torrie and J.-P. Valleau, J. Comput. Phys. **23**, 187 (1977).

[5] R. H. Swendsen and J.-S. Wang, Phys. Rev. Lett. **57**, 2607 (1986).

[6] C. J. Geyer, in *Computing Science and Statistics: Proceedings of the 23rd Symposium on the Interface*, edited by E. K. Keramidas (Interface Foundation, Fairfax Station, New York, 1991), p. 156.

[7] E. Marinari and G. Parisi, Europhys. Lett. **19**, 1604 (1992).

[8] A. P. Lyubartsev, A. A. Martsinovski, S. V. Shevkunov, and P. N. Vorontsov-Velyaminov, J. Chem. Phys. **96**, 1776 (1992).

[9] K. Hukushima and K. Nemoto, J. Phys. Soc. Jpn. **65**, 1604 (1996).

[10] E. Marinari, G. Parisi, and J. Ruiz-Lorenzo, in *Spin Glasses and Random Fields*, edited by A. Young, Directions in Condensed Matter Physics Vol. 12 (World Scientific, Singapore, 1998).

[11] P. M. C. Oliveira, T. J. P. Penna, and H. J. Herrmann, Braz. J. Phys. **26**, 677 (1996).

[12] B. A. Berg and T. Neuhaus, Phys. Lett. B **267**, 249 (1991).

[13] B. A. Berg and T. Celik, Int. J. Mod. Phys. C **3**, 1251 (1992).

[14] J. Lee, Phys. Rev. Lett. **71**, 211 (1993).

[15] J.-S. Wang and R. H. Swendsen, J. Stat. Phys. **106**, 245 (2002).

[16] F. Wang and D. P. Landau, Phys. Rev. Lett. **86**, 2050 (2001).

[17] F. Wang and D. P. Landau, Phys. Rev. E **64**, 056101 (2001).

[18] B. J. Schulz, K. Binder, and M. Müller, Int. J. Mod. Phys. C **13**, 477 (2002).

[19] N. Douarche, F. Calvo, G. M. Pastor, and P. J. Jensen, Eur. Phys. J. D **24**, 77 (2003).

[20] M. Troyer, S. Wessel, and F. Alet, Phys. Rev. Lett. **90**, 120201 (2003).

[21] A. Malakis, A. Peratzakis, and N. G. Fytas, Phys. Rev. E **70**, 066128 (2004).

[22] G. Brown and T. C. Schuthess, J. Appl. Phys. **97**, 10E303 (2005).

[23] B. J. Schulz, K. Binder, and M. Müller, Phys. Rev. E **71**, 046705 (2005).

[24] S. Reynal and H. T. Diep, Phys. Rev. E **72**, 056710 (2005).

[25] A. Malakis, S. S. Martinos, I. A. Hadjiagapiou, N. G. Fytas, and P. Kalozoumis, Phys. Rev. E **72**, 066120 (2005).

[26] D. Jayasri, V. S. S. Sastry, and K. P. N. Murthy, Phys. Rev. E **72**, 036702 (2005).

[27] Q. Yan, R. Faller, and J. J. de Pablo, J. Chem. Phys. **116**, 8745 (2002).

[28] M. S. Shell, P. G. Debenedetti, and A. Z. Panagiotopoulos, Phys. Rev. E **66**, 056703 (2002).

[29] Q. Yan and J. J. de Pablo, Phys. Rev. Lett. **90**, 035701 (2003).

[30] M. Fasnacht, R. H. Swendsen, and J. M. Rosenberg, Phys. Rev. E **69**, 056704 (2004).

[31] S. Trebst, E. Gull, and M. Troyer, J. Chem. Phys. **123**, 204501 (2005).

[32] N. Rathore and J. J. de Pablo, J. Chem. Phys. **116**, 7225

(2002).

[33] N. Rathore, T. A. Knotts IV, and J. J. de Pablo, J. Chem. Phys. **118**, 4285 (2003).

[34] N. Rathore, G. Yan, and J. J. de Pablo, J. Chem. Phys. **120**, 5781 (2004).

[35] V. Varshney, T. E. Dirama, T. Z. Sen, and G. A. Carri, Macromolecules **37**, 8794 (2004).

[36] V. Varshney and G. A. Carri, Phys. Rev. Lett. **95**, 168304 (2005).

[37] G. A. Carri, R. Batman, V. Varshney, and T. E. Dirama, Polymer **46**, 3809 (2005).

[38] F. Calvo, Mol. Phys. **100**, 3421 (2002).

[39] F. Calvo and P. Parneix, J. Chem. Phys. **119**, 256 (2003).

[40] R. Faller and J. J. de Pablo, J. Chem. Phys. **119**, 4405 (2003).

[41] M. S. Shell, P. G. Debenedetti, and A. Z. Panagiotopoulos, J. Chem. Phys. **119**, 9406 (2003).

[42] B. J. Schulz, K. Binder, M. Müller, and D. P. Landau, Phys. Rev. E **67**, 067102 (2003).

[43] C. Zhou and R. N. Bhatt, Phys. Rev. E **72**, 025701(R) (2005).

[44] A. Tröster and C. Dellago, Phys. Rev. E **71**, 066705 (2005).

[45] J. P. K. Doye, M. A. Miller, and D. J. Wales, J. Chem. Phys. **111**, 8417 (1999).

[46] C. Zhou, T. C. Schulthess, S. Torbrügge, and D. P. Landau, Phys. Rev. Lett. **96**, 120201 (2006).

[47] S. Kirkpatrick, C. D. Gelatt, and M. P. Vecchi, Science **220**, 671 (1983).

[48] A. M. Ferrenberg and R. H. Swendsen, Phys. Rev. Lett. **63**, 1195 (1989).

[49] Y. Sugita, A. Kitao, and Y. Okamoto, J. Chem. Phys. **113**, 6042 (2000).

[50] A. Mitsutake, Y. Sugita, and Y. Okamoto, Biopolymers **60**, 96 (2001).

[51] D. A. Kofke, J. Chem. Phys. **117**, 6911 (2002).

[52] K. Sanbonmatsu and A. E. García, Proteins: Struct., Funct., Genet. **46**, 225 (2002).

[53] S. Kumar, D. Bouzida, R. H. Swendsen, P. A. Kollman, and J. M. Rosenberg, J. Comput. Chem. **13**, 1011 (1992).

[54] M. R. Shirts and V. S. Pande, Science **290**, 1903 (2000).

[55] E. J. Sorin and V. S. Pande, J. Comput. Chem. **26**, 682 (2005).

[56] P. Dugourd, R. Antoine, G. Breaux, M. Broyer, and M. F. Jarrold, J. Am. Chem. Soc. **127**, 4675 (2005).

[57] T. Tabarin, R. Antoine, M. Broyer, and P. Dugourd, Rapid Commun. Mass Spectrom. **19**, 2883 (2005).

[58] R. Antoine, M. Broyer, J. Chamot-Rooke, C. Dedonder, C. Desfrançois, P. Dugourd, G. Grégoire, C. Jouvet, P. Poulain, T. Tabarin, and G. van der Rest, Rapid Commun. Mass Spectrom.

20, 1648 (2006).

[59] S. J. Weiner, P. A. Kollman, D. A. Case, U. C. Singh, C. Ghio, G. Alagona, S. Profeta, Jr., and P. K. Weiner, J. Am. Chem. Soc. **106**, 765 (1984).

[60] P. Kollman, R. Dixon, W. Cornell, T. Fox, C. Chipot, and A. Pohorille, in *Computer Simulations of Biomolecular Systems*, edited by W. F. van Gunsteren, P. K. Weiner, and A. J. Wilkinson (Kluwer, Dordrecht, 1997).

[61] U. H. E. Hansmann and Y. Okamoto, J. Chem. Phys. **110**, 1267 (1999); **111**, 1339 (1999) (E).

[62] Y. Peng and U. H. E. Hansmann, Biophys. J. **82**, 3269 (2002).

[63] D. D. Frantz, D. L. Freeman, and J. D. Doll, J. Chem. Phys. **93**, 2769 (1990).

[64] J. Ma and J. E. Straub, J. Chem. Phys. **101**, 533 (1994).

[65] D. J. Wales and J. P. K. Doye, J. Phys. Chem. A **101**, 5111 (1997).

[66] F. Calvo, J. Chem. Phys. **123**, 124106 (2005).

[67] J. P. K. Doye, M. A. Miller, and D. J. Wales, J. Chem. Phys. **111**, 8417 (1999).

[68] F. Calvo and J. P. K. Doye, Phys. Rev. E **63**, 010902(R) (2000).

[69] D. D. Frantz, J. Chem. Phys. **115**, 6136 (2002).

[70] D. Sabo, D. L. Freeman, and J. D. Doll, J. Chem. Phys. **122**, 094716 (2005).

[71] H. Liu and K. D. Jordan, J. Phys. Chem. A **109**, 5203 (2005).

[72] J. P. Neirotti, F. Calvo, D. L. Freeman, and J. D. Doll, J. Chem. Phys. **112**, 10340 (2000).

[73] V. A. Mandelshtam, P. A. Frantsuzov, and F. Calvo, J. Phys. Chem. A **110**, 5326 (2006).

[74] J. P. K. Doye and F. Calvo, J. Chem. Phys. **116**, 8307 (2002).

[75] J. A. Northby, J. Chem. Phys. **87**, 6166 (1987).

[76] P. J. Steinhardt, D. R. Nelson, and M. Ronchetti, Phys. Rev. B **28**, 784 (1983).

[77] J. P. K. Doye and D. J. Wales, Phys. Rev. Lett. **80**, 1357 (1998).

[78] J. P. K. Doye, M. A. Miller, and D. J. Wales, J. Chem. Phys. **110**, 6896 (1999).

[79] P. A. Frantsuzov and V. A. Mandelshtam, Phys. Rev. E **72**, 037102 (2005).

[80] P. Dayal, S. Trebst, S. Wessel, D. Würtz, M. Troyer, S. Sabhapandit, and S. N. Coppersmith, Phys. Rev. Lett. **92**, 097201 (2004).

[81] M. S. Shell, P. G. Debenedetti, and A. Z. Panagiotopoulos, J. Phys. Chem. **108**, 19748 (2004).

[82] M. D. Costa, J. Viana Lopes, and J. M. B. Lopes dos Santos, Europhys. Lett. **72**, 802 (2005).